© 2014. Published by The Company of Biologists Ltd | Journal of Cell Science (2014) 127, 1117–1127 doi:10.1242/jcs.143750

RESEARCH ARTICLE

The $A\beta_{1-42}$ peptide regulates microtubule stability independently of tau

Barbara Pianu[1,§], Roger Lefort[1,§], Laure Thuiliere[1,2], Elsa Tabourier[1,*] and Francesca Bartolini[1,¶]

ABSTRACT

Interference with microtubule stability by beta-amyloid peptide (Aβ) has been shown to disrupt dendritic function and axonal trafficking, both early events in Alzheimer's disease. However, it is unclear whether Aβ regulation of microtubule dynamics can occur independently of its action on tau. RhoA has been implicated in neurotoxicity by Aβ but the mechanism by which this activation generates cytoskeletal changes is also unclear. We found that oligomeric $A\beta_{1-42}$ induced the formation of stable detyrosinated microtubules in NIH3T3 cells and this function resulted from the activation of a RhoA-dependent microtubule stabilization pathway regulated by integrin signaling and the formin mDia1. Induction of microtubule stability by Aβ was also initiated by dimerization of APP and required caspase activity, two previously characterized regulators of neurotoxicity downstream of Aβ. Finally, we found that this function was conserved in primary neurons and abolished by Rho inactivation, reinforcing a link between induction of stable detyrosinated microtubules and neuropathogenesis by Aβ. Our study reveals a novel activity of Aβ on the microtubule cytoskeleton that is independent of tau and associated with pathways linked to microtubule stabilization and Aβ-mediated neurotoxicity.

KEY WORDS: Amyloid beta, Aβ, $A\beta_{1-42}$ peptide, Stable microtubules, RhoA, Integrin signaling, mDia1, Caspase, APP

INTRODUCTION

Compelling evidence suggests that Alzheimer's disease (AD) is caused by increased amyloidogenic processing of the amyloid precursor protein (APP), leading to elevated levels of the APP-derived beta-amyloid peptide (Aβ) and formation of amyloid plaques. These changes are accompanied by the formation of neurofibrillary tangles (NFTs), composed of the microtubule (MT)-associated protein (MAP) tau, loss of synaptic function, neuritic dystrophy and eventually cell death. As tau in NFTs is hyperphosphorylated and binds poorly to MTs, a predominant model is that Aβ overproduction causes tau hyperphosphorylation and its relocation into a dendritic compartment, resulting in MT destabilization and neuronal damage (Busciglio et al., 1995; Ferreira et al., 1997; Ittner and Götz, 2011; LaFerla, 2010; Takashima et al., 1996; Takashima et al., 1993; Takashima et al., 1995; Zheng et al., 2002).

Despite the large amount of data supporting the 'Aβ to tau' hypothesis in the induction of neurotoxicity in AD, the steps that connect Aβ to tau have remained poorly defined (Ittner and Götz, 2011). A mechanism yet to be tested is that Aβ first deregulates MT stability, which leads to tau hyperphosphorylation as a cellular response to compensate for changes in MT behavior. In non-neuronal cells that do not express tau, Aβ has been shown to impair the assembly and maintenance of the mitotic spindle through inhibition of mitotic motor kinesins (Borysov et al., 2011). However, Aβ has also been reported to disrupt the integrity of non-mitotic MT arrays of non-neuronal cells in the presence of tau (King et al., 2006). Surprisingly, it has never been tested whether Aβ can regulate MT dynamics or MT post-translational modifications of non-mitotic MT arrays in the absence of tau.

Deregulation of Rho GTPase signaling has been implicated in neurotoxicity by Aβ (Chacon et al., 2011; Petratos et al., 2008; Pozueta et al., 2013). Alterations in actin dynamics is generally considered the mechanism by which Rho contributes to the collapse of dendritic spines and impairs synaptic transmission, all early events occurring in neurons exposed to Aβ (Lambert et al., 1998; Lefort et al., 2012; Lesné et al., 2006; Nimmrich and Ebert, 2009; Shankar et al., 2007). However, it is not known whether neurotoxicity might also derive from changes in MT dynamics and/or MT post-translational modifications induced by Rho activation through the action on its effector mDia1 (Goulimari et al., 2005; Palazzo et al., 2001a). In neurons, APP and caspase-2 can regulate RhoA activation, and cells lacking either APP or caspase-2 are completely immune to Aβ synaptotoxicity (Pozueta et al., 2013; Troy et al., 2000). In addition, dimerization of cell-surface APP by cross-linking cell-surface APP with a divalent antibody is sufficient to mimic the toxic effects of Aβ in neurons (Lefort et al., 2012; Rohn et al., 2000). Interestingly, activation of RhoA in neuronal cells by lysophosphatidic acid (LPA) is also regulated by caspase-2 activity, suggesting that Aβ and LPA share pathways (Pozueta et al., 2013).

In migrating fibroblasts, a signaling cascade downstream of LPA and integrin activation regulates the formation of a polarized subset of stable detyrosinated MTs through RhoA (Bartolini and Gundersen, 2010; Bartolini et al., 2008; Bartolini et al., 2012; Cook et al., 1998; Eng et al., 2006; Goulimari et al., 2005; Goulimari et al., 2008; Gundersen et al., 1994; Nagasaki and Gundersen, 1996; Palazzo et al., 2001a; Palazzo et al., 2004; Wen et al., 2004). This class of MTs is believed to provide stable tracks for the delivery of actin and focal adhesion regulators to the protruding leading edge. MT detyrosination is a tubulin post-translation modification associated with stable MTs that results in the exposure of a glutamic acid residue in the C-terminal region of an α-tubulin subunit (Gundersen et al., 1984; Hallak et al.,

[1]Department of Pathology and Cell Biology, Columbia University, New York, NY, 10032, USA. [2]AgroParisTech, 16 Rue Claude Bernard 75005 Paris, France.

*Present address: Mondelez International, 13 Avenue Morane Saulnier, 78140 Vélizy-Villacoublay, France.

[§]These authors contributed equally to the work.

[¶]Author for correspondence (fb2131@columbia.edu)

Received 1 October 2013; Accepted 11 December 2013

Journal of Cell Science (2014) 127, 1117–1127 doi:10.1242/jcs.143750

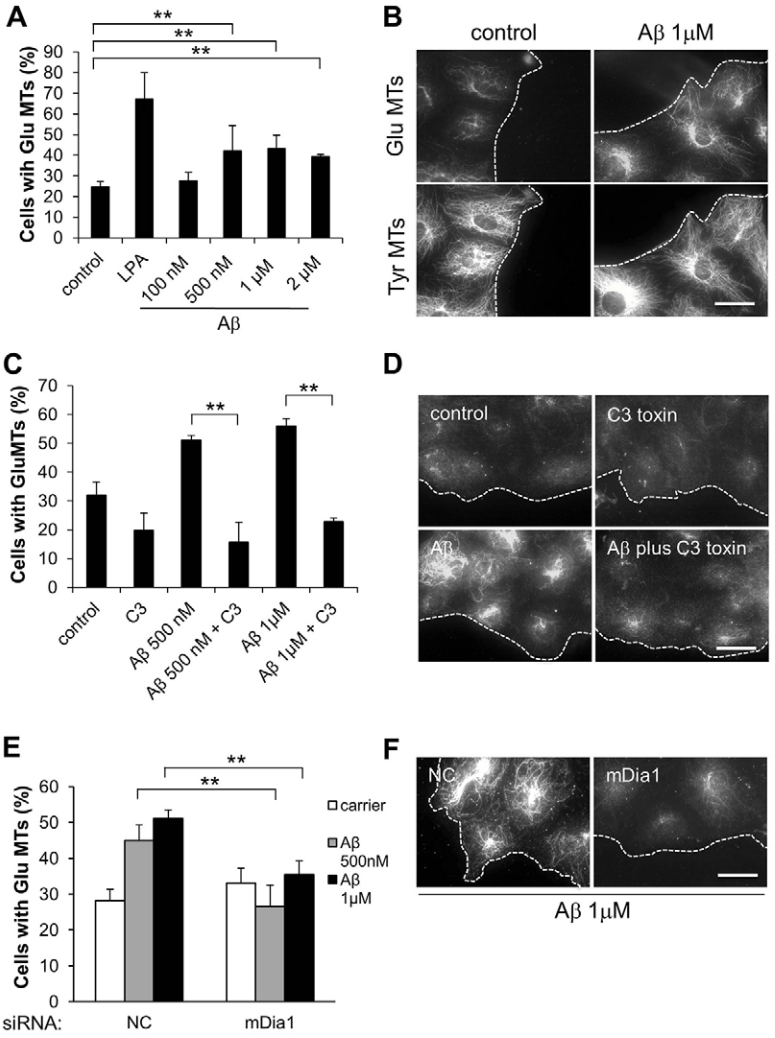

Fig. 1. Aβ induces stable Glu MTs through the Rho/mDia1 stabilization pathway. (A) The percentage of cells with Glu MTs after incubation with oligomeric $A\beta_{1\text{-}42}$. (B) Immunostaining using primary antibodies against detyrosinated or tyrosinated tubulin, Glu MTs and Tyr MTs, respectively, in cells at the wound treated as in A. (C) The percentage of cells with Glu MTs after incubation with the toxin C3 prior to treatment with oligomeric $A\beta_{1\text{-}42}$. (D) Immunostaining for detyrosinated tubulin (Glu) in cells at the wound treated as in C. (E) The percentage of cells with Glu MTs after silencing for mDia1 expression by siRNA prior to incubation with oligomeric $A\beta_{1\text{-}42}$. NC, control siRNA. (F) Immunostaining for detyrosinated tubulin (Glu) in cells at the wound treated as in (E). Data are means from three independent experiments ($n>100$ per sample in each experiment). $^{**}P<0.01$ (Chi-squared test). Scale bars: 20 μm.

1977). We refer to this population of stable detyrosinated MTs as Glu MTs, to distinguish them from tyrosinated MTs (Tyr MTs) that are dynamic (Schulze et al., 1987; Schulze and Kirschner, 1987). MT detyrosination has been shown to abolish the plus-end tracking of CAP glycine proteins (Peris et al., 2006), inhibit MT depolymerization by kinesin-13 family motors (Peris et al., 2009) and increase the affinity of conventional kinesin to MTs (Dunn et al., 2008; Konishi and Setou, 2009; Kreitzer et al., 1999; Liao et al., 1999). In fibroblasts, the LPA and integrin pathway activates RhoA, which in turn acts through the formin mDia1 and several MT- and actin-binding proteins to capture and directly stabilize MTs at cortical sites (Andrés-Delgado et al., 2012; Bartolini and Gundersen, 2010; Bartolini et al., 2008; Bartolini et al., 2012; Cook et al., 1998; Eng et al., 2006; Goulimari et al., 2005; Goulimari et al., 2008; Gundersen et al., 1994; Nagasaki and Gundersen, 1996; Palazzo et al., 2001a; Palazzo et al., 2004; Wen et al., 2004). MT stabilization by the formin mDia1 is thought to be dependent on the interaction of mDia1 with MTs and with several MT-plus-end-binding proteins (Bartolini and Gundersen, 2010; Bartolini et al., 2008; Wen et al., 2004). mDia1 might also indirectly affect MT stability because it is necessary for the PKC-dependent phosphorylation of GSK3β (Eng et al., 2006), a ubiquitously expressed serine/threonine kinase that plays a key role in the pathogenesis of AD by hyperphosphorylating tau in most serine and threonine residues, and by contributing both to Aβ production and Aβ-mediated neuronal death (Hernandez et al., 2013).

In order to segregate tau-dependent from tau-independent effects, we examined whether Aβ could induce stable Glu MTs through a RhoA-mediated mechanism in cells that naturally do not express tau. Immortalized NIH3T3 cultures were chosen for this study because MT stability can be rapidly and reliably quantified using indirect immunofluorescence, and the molecular pathway leading to MT stabilization downstream of RhoA signaling has been extensively characterized in these cells (Bartolini and Gundersen, 2010; Bartolini et al., 2008; Bartolini et al., 2012; Cook et al., 1998; Eng et al., 2006; Goulimari et al., 2005; Goulimari et al., 2008; Gundersen et al., 1994; Palazzo et al., 2001a; Palazzo et al., 2004; Wen et al., 2004).

Here, we found that short exposures to neurotoxic concentrations of oligomeric $A\beta_{1\text{-}42}$ induced the formation of stable Glu MTs in serum-starved NIH3T3 cells in a RhoA- and mDia1-dependent manner. This function was regulated by integrin signaling, APP dimerization and caspase activity, thereby linking regulation of MT stability to pathways involved in Aβ-mediated neurotoxicity. Importantly, Rho-dependent induction of increased Glu MT levels was also detected in primary neurons exposed to Aβ, demonstrating that the pathways that lead to stable detyrosinated microtubules by Aβ are conserved and possibly contribute to neuropathogenesis.

Journal of Cell Science (2014) 127, 1117–1127 doi:10.1242/jcs.143750

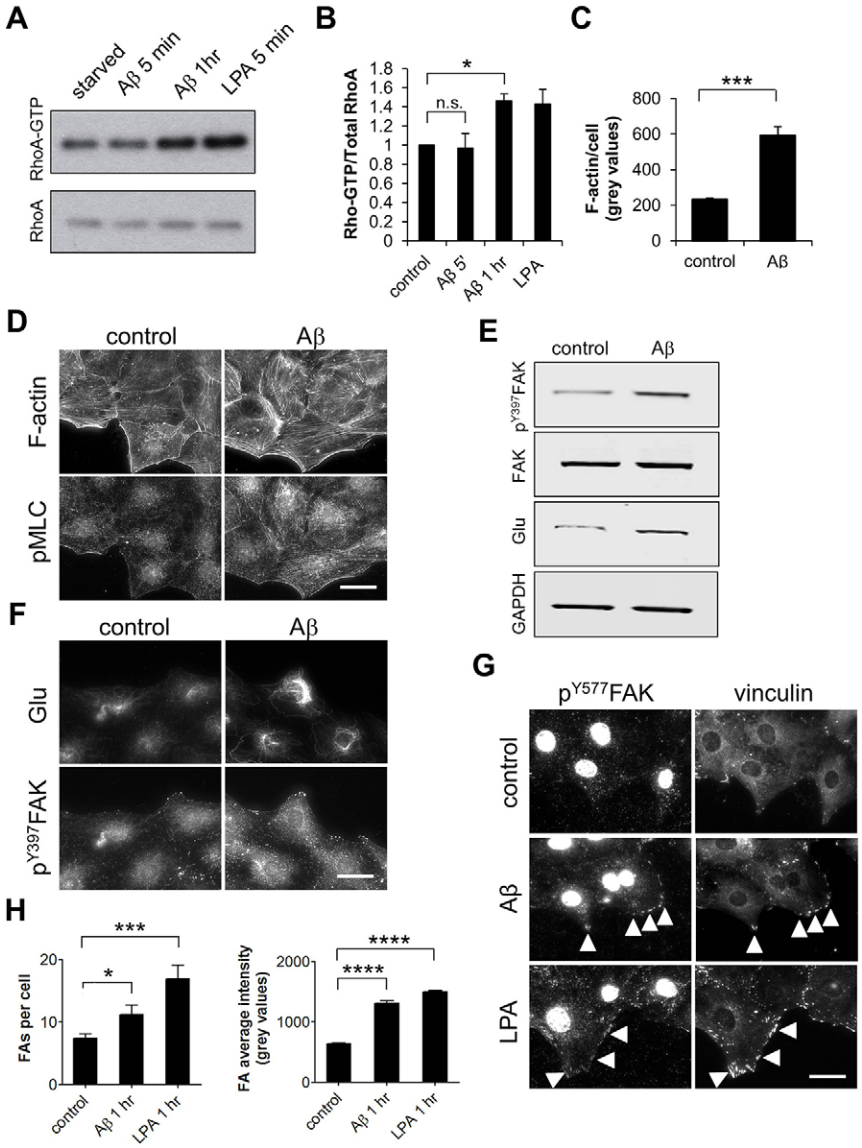

Fig. 2. Aβ induces active RhoA and focal adhesion assembly. (A) Western blot analysis of RhoA-GTP pull-down reactions from starved cells treated with Aβ (1 μM) or LPA (10 μM). A specific antibody against RhoA was used to detect both RhoA-GTP and total RhoA levels from input lysates (the bottom panel shows 8% of the input lysate for each condition). (B) Quantification of the ratio between RhoA-GTP and total RhoA levels in cells treated as in A. (C) Quantification of the levels of F-actin measured by phalloidin staining in starved cells incubated with Aβ (1 μM) for 1 h. (D) Fluorescent phalloidin and phospho-myosin-light chain (pMLC) immunostaining of cells at the wound for cells treated as in C. (E) Western blot analysis of starved cells treated with vehicle (control) or Aβ (1 μM) for 1 h prior to lysis. Total FAK, p^{Y397}FAK, detyrosinated tubulin (Glu) and GAPDH levels (as a loading control) were detected using specific antibodies. (F) Immunostaining for detyrosinated tubulin (Glu) and p^{Y397}FAK primary antibodies in cells at the wound treated as in E. (G) Immunostaining using vinculin and p^{Y577}FAK in cells at the wound treated as in E, and plus LPA (10 μM). Arrowheads show focal adhesions (FAs). (H) Quantification of number of FAs per cell and focal adhesion average intensity by measuring vinculin immunostaining in cells at the wound treated as in G. Data are means±s.e.m. from three independent experiments. *$P<0.05$, ***$P<0.001$, **** $P<0.0001$ by Student's *t*-test. Scale bars: 20 μm.

RESULTS

Soluble oligomeric $Aβ_{1-42}$ induces stable Glu MTs through the Rho/mDia pathway

Serum-starved NIH3T3 cells deprived of stable MTs and naturally lacking tau expression were exposed to soluble oligomeric $Aβ_{1-42}$ (Stine et al., 2003) for 2 h prior to fixation. We found that oligomeric Aβ induced Glu MTs above the levels in starved cells yet below those triggered by LPA (Fig. 1A,B). Glu MT induction by Aβ was greatest at 0.5–1 μM Aβ, becoming inhibited at higher concentrations, presumably owing to cell toxicity. The stability of Glu MTs induced by Aβ was confirmed by their resistance to nocodazole-induced depolymerization followed by brief saponin extraction under conditions that preserved the MT polymer, and by staining of acetylated tubulin, another post-translational modification associated with MT longevity (supplementary material Fig. S1). Pre-incubation with the toxin C3, which specifically inhibits Rho, dramatically reduced the percentage of cells with Glu MTs induced by Aβ (Fig. 1C,D). We explored the possibility that induction of stable Glu MTs by Aβ was accomplished through the Rho effector mDia1, which is also implicated in MT stabilization by LPA (Goulimari et al., 2005; Palazzo et al., 2001a), and silenced the expression of mDia1 by siRNA transfection prior to Aβ incubation. Knockdown of mDia1 expression was sufficient to significantly dampen the induction of MT stability by Aβ, indicating that Aβ activates the Rho/mDia1 MT stabilization pathway (Fig. 1E,F). Specificity of Aβ acting through the Rho pathway rather than the Cdc42 pathway, which regulates MTOC positioning and nuclear movement in polarizing cells (Gomes et al., 2005; Palazzo et al., 2001b), was further supported by the lack of centrosome reorientation towards the leading edge in starved cells treated with Aβ after wounding (supplementary material Fig. S2). These data demonstrate a novel activity for Aβ in inducing a subset of stable MTs through the activation of a defined pathway downstream of Rho.

Aβ activates RhoA and FAK activities

By analogy with LPA, RhoA activation was tested and measured by using quantitative western blot analysis of GST-Rhotekin pull-down assays from serum-starved cells treated with Aβ or LPA (Fig. 2A,B). We found that whereas LPA lead to a rapid and robust activation of RhoA at 5 min, Aβ induced comparable levels of RhoA GTP after 1 h, indicating slower kinetics of activation.

Journal of Cell Science (2014) 127, 1117–1127 doi:10.1242/jcs.143750

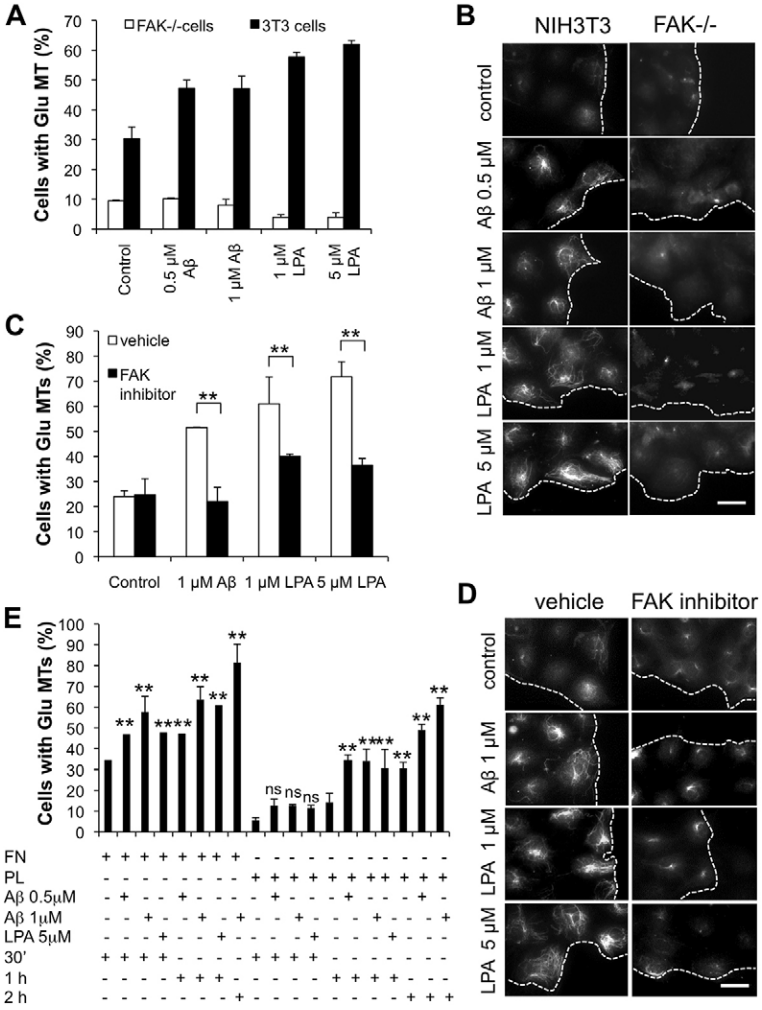

Fig. 3. Integrin signaling and FAK are required for Aβ-mediated induction of Glu MTs. (A) The percentage of NIH3T3 or FAK$^{-/-}$ cells with Glu MTs after incubation with oligomeric A$\beta_{1\text{-}42}$ or LPA. (B) Immunostaining for detyrosinated tubulin (Glu) in cells at the wound treated as in A. (C) The percentage of cells with Glu MTs after incubation with the FAK inhibitor (PF228) 30 min prior to treatment with oligomeric A$\beta_{1\text{-}42}$ or LPA. (D) Immunostaining for detyrosinated tubulin (Glu) in cells at the wound treated as in C. (E) The percentage of resuspended cells with Glu MTs cells after cells were allowed to spread on polylysine (PL) or fibronectin (FN) for 30 min, 1 h or 2 h, in the presence of oligomeric A$\beta_{1\text{-}42}$ or LPA. Data are means±s.e.m. from three independent experiments (n>100 per sample in each experiment). **P<0.01 (Chi-squared test); ns, not significant. Scale bars: 20 μm.

We evaluated whether the increase in RhoA activity in cells treated with Aβ corresponded to an increase in actin polymerization and myosin-mediated contraction, as is the case for LPA (Chrzanowska-Wodnicka and Burridge, 1996). Quantification of F-actin levels by measurements of phalloidin staining showed a threefold increase after incubation with Aβ (Fig. 2C,D). The same cells also appeared to induce actomyosin-mediated contractility as indicated by a substantial increase in phospho-myosin light chain immunostaining (Fig. 2D). In addition, we found that Aβ induced phosphorylation of FAK at Y397 (p^{Y397}FAK) and focal adhesion assembly (Fig. 2E–H). p^{Y577}FAK, another marker of newly formed focal adhesions, also appeared upregulated in cells treated with Aβ or LPA, suggesting induction of full FAK kinase activity caused by Src phosphorylation (Playford and Schaller, 2004) (Fig. 2G). We measured the induction of focal adhesion assembly, estimated by the amount and intensity of vinculin staining, and found it significantly increased by Aβ, yet lower than the increase with LPA (Fig. 2H). These data demonstrate that Aβ is a genuine yet slow activator of RhoA, leading to induction of F-actin levels, FAK activity and focal adhesion assembly.

Integrin signaling and FAK are required for Aβ induction of Glu MTs

We examined whether cell adhesion and integrin signaling through FAK were crucial for Aβ induction of stable Glu MTs (Palazzo et al., 2004). Both Aβ and LPA failed to induce Glu MTs in FAK$^{-/-}$ cells (Ilić et al., 1995) or in wild-type cells pre-incubated with a specific FAK inhibitor prior to LPA or Aβ treatment (Fig. 3A–D). Moreover, no significant induction of Glu MTs was scored above background levels in wild-type cells plated on poly-lysine and treated with Aβ or LPA after 30 min, whereas both treatments induced Glu MTs in wild-type cells re-plated on fibronectin (Fig. 3E; supplementary material Fig. S3). Induction of Glu MTs on poly-lysine resumed at later time points (1 h and 2 h) presumably when cells began to secrete their own fibronectin. From these results, we conclude that cell adhesion and integrin signaling through FAK are necessary for Aβ to form Glu MTs.

APP signaling is required for Aβ induction of Glu MTs

Given the direct involvement of APP with both cell adhesion and neuronal injury by Aβ (Sabo et al., 2001; Xu et al., 2009; Yamazaki et al., 1997), we tested whether stimulation of APP signaling was also required to induce stable Glu MTs by Aβ. Interestingly, downregulation of APP expression prior to Aβ treatment completely abrogated the induction of stable Glu MTs by Aβ (Fig. 4A–C). We tested whether APP signaling was sufficient to induce Glu MTs and stimulated APP dimerization by treating serum-starved cells with a cross-linking APP antibody (22C11) (Lefort et al., 2012) (Fig. 4D,E). We observed a significant increase in MT stability in cells that were treated with intact 22C11, whereas Glu MT levels in cells treated with the monovalent Fab fragment of 22C11 remained virtually unchanged, reinforcing the notion that Aβ and APP signal through the same pathway(s).

Journal of Cell Science (2014) 127, 1117–1127 doi:10.1242/jcs.143750

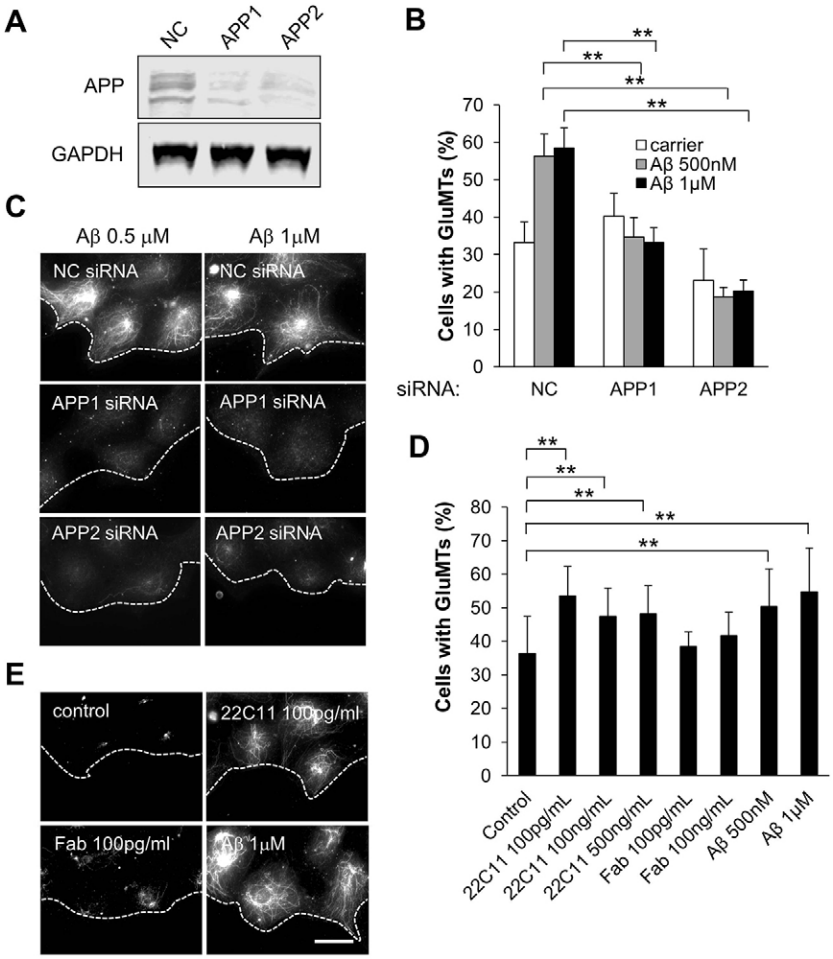

Fig. 4. Expression of APP and its dimerization are crucial for Aβ induction of Glu MTs. (A) Western blot analysis of APP levels in control cells (NC) and in cells silenced for APP using two distinct siRNAs (APP1 and APP2). GAPDH levels are also shown (as a loading marker). (B) The percentage of cells with Glu MTs after silencing for the expression of APP by two independent siRNAs (APP1 and APP2) followed by incubation with oligomeric $A\beta_{1\text{-}42}$. (C) Immunostaining for detyrosinated tubulin (Glu) in cells at the wound treated as in B. (D) The percentage of cells with Glu MTs after incubation with a range of concentrations of 22C11 antibody or the isolated monovalent Fab fragments of 22C11. (E) Immunostaining for detyrosinated tubulin (Glu) in cells at the wound treated as in D. Data are means±s.e.m. from three independent experiments ($n>100$ per sample in each experiment). $^{**}P<0.01$ (Chi-squared test). Scale bars: 20 μm.

Aβ induction of Glu MTs is mediated by caspase activity

Activation of RhoA by LPA and Aβ in neurons is regulated by caspase-2 activity, suggesting that Aβ and LPA share effectors (Pozueta et al., 2013). In addition, longer exposures of starved NIH3T3 cells to Aβ resulted in a significant increase in cell mortality indicating that activation of death pathways by Aβ also occurs in non-neuronal cells (supplementary material Fig. S4). We found that wide-spectrum inhibition of caspase activity with the pan-caspase inhibitor Z-VAD completely abrogated the formation of stable Glu MTs by both Aβ and LPA treatments (Fig. 5A,B). Pre-treatment of cells with chemical inhibitors against four different caspases showed that the activities of caspase-2 and -3 and to a lesser degree caspase-9, but not caspase-6, were necessary for Aβ-mediated induction of stable Glu MTs in NIH3T3 (Fig. 5C,E). Owing to the weak specificity of chemical caspase inhibitors, in the case of caspases-2 or -3, both widely implicated in neurodamage by Aβ (D'Amelio et al., 2011; Hyman, 2011; Pozueta et al., 2013; Troy et al., 2000), the results were confirmed by silencing the expression with specific siRNA oligonucleotides prior to Aβ treatment (Fig. 5D,E). Taken together, these results demonstrate that RhoA, APP and caspase-2 and -3 all act downstream of Aβ to induce stable Glu MTs.

Aβ induces Glu MTs in cultured primary neurons through Rho activity

We tested whether short exposures to Aβ oligomers induced localized changes in Glu MT levels in primary hippocampal neurons. Because in differentiated neurons the neuronal processes are packed with stable MTs that are hard to distinguish from the dynamic ones, the best way to assess relative abundance of different classes of MTs in neurites is to perform ratio measurements between the chosen class of modified MTs (in our case detyrosinated or Glu MTs) and a bulk marker of MTs (DM1A). We found that a 3 h exposure to oligomeric $A\beta_{1\text{-}42}$ did not cause substantial variations in cell morphology but was sufficient to induce a significant increase in the ratio between detyrosinated and total MT levels in individual neurite segments (Fig. 6A–D). Next, we tested whether this increase was dependent on RhoA activation by measuring the Glu-MT:DM1A ratio in neurons challenged with the specific Rho inhibitor C3 prior to incubation with Aβ or in neurons incubated with the RhoA activator LPA. We found that pre-incubations with C3 toxin were sufficient to significantly dampen the induction of Glu MTs by Aβ (Fig. 6E,F) whereas exposures to LPA caused an increase in the Glu-MT:DM1A ratio in individual neurites to an extent comparable to that by Aβ (Fig. 6G,H). These findings suggest that the pathways that lead to Glu MTs formation by Aβ are conserved in neurons and that a primary function of Aβ is to modify a population of stable MTs prior to neurite degeneration.

DISCUSSION

In this study, we have found that neurotoxic concentrations of oligomeric $A\beta_{1\text{-}42}$ induced the formation of stable Glu MTs in non-neuronal cells and in primary neurons. Initial characterization of the signaling in fibroblasts showed that Glu MTs were generated through

Journal of Cell Science (2014) 127, 1117–1127 doi:10.1242/jcs.143750

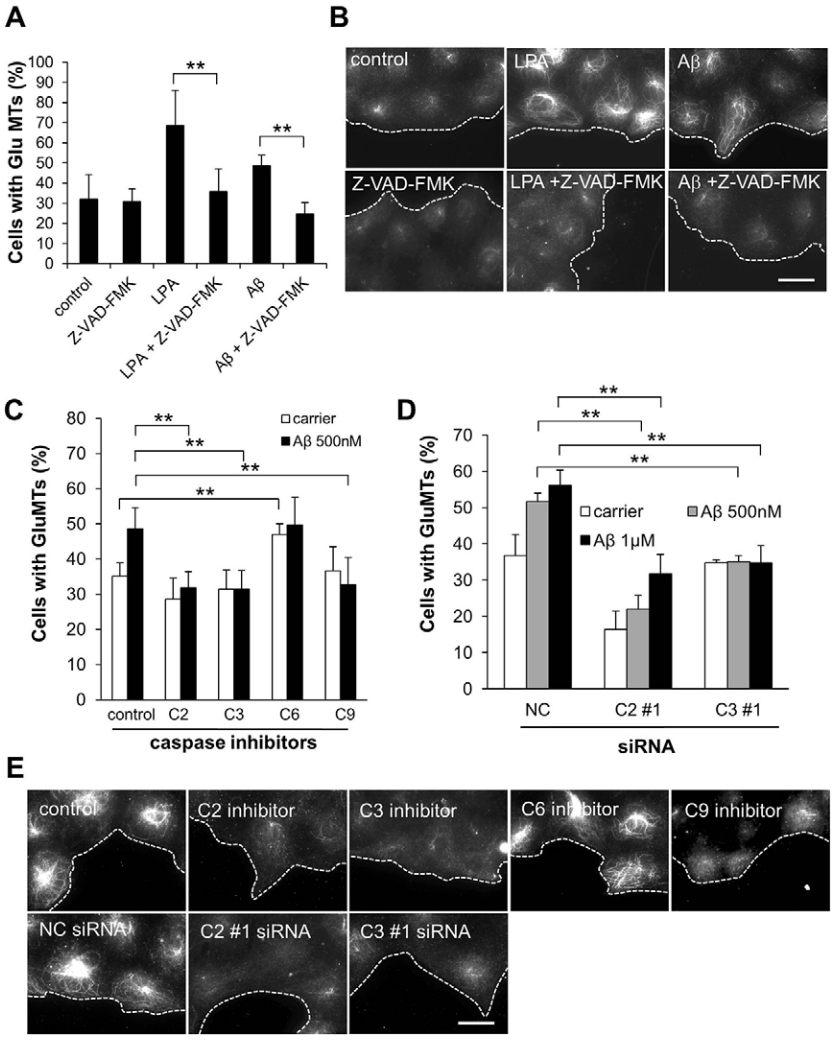

Fig. 5. Aβ induction of Glu MTs is mediated by caspase activities. (A) The percentage of cells with Glu MTs after incubation for 30 min with a pan-caspase inhibitor (Z-VAD-FMK) (10 μM) prior to treatment with oligomeric $Aβ_{1-42}$ (1 μM) or LPA (5 μM). (B) Immunostaining for detyrosinated tubulin (Glu) in cells at the wound treated as in A. (C) The percentage of cells with Glu MTs after incubation for 30 min with inhibitors specific for caspase-2, -3, -6 and -9 (10 μM) prior to treatment with oligomeric $Aβ_{1-42}$ (0.5 μM). (D) The percentage of cells with Glu MTs after silencing for caspase-2 and -3 expression by siRNA oligoduplex transfection (C2#1 for caspase-2 and C3#1 for caspase-3) prior to incubation with oligomeric $Aβ_{1-42}$. (E) Immunostaining for detyrosinated tubulin (Glu) in cells at the wound treated as in C and D. Data are means±s.e.m. from three independent experiments ($n>100$ per sample in each experiment). $^{**}P<0.01$ (Chi-squared test). Scale bars: 20 μm.

RhoA and its effector mDia1. These are surprising results that reveal a conserved function of Aβ on the MT cytoskeleton independently of tau expression and suggest that a primary activity of Aβ is to regulate the stabilization rather than the destabilization of MTs and to modify the levels of tubulin detyrosination, which is associated with MT longevity. The role of the formin mDia1 is also intriguing given the crucial roles that formins play in the regulation of the actin and MT cytoskeletons (Bartolini and Gundersen, 2010; Chesarone et al., 2010) and that virtually nothing is known of the function of mDia1 on the dynamics of the MT cytoskeleton in the adult brain or at the onset of neuronal damage.

We found that Aβ induced RhoA-GTP, FAK activation and focal adhesion assembly. In addition, we observed a significant increase in the levels of F-actin and phospho-myosin light chain after treatment with Aβ. By analogy with LPA, we speculate that active FAK is required for RhoA-mediated mDia1 activation by Aβ. However, whether FAK activation is dependent solely on RhoA-GTP or whether it is partially a result of Aβ-mediated stimulation of integrin signaling remains to be elucidated (see Fig. 7).

A functional link between Aβ and integrins or FAK signaling has also been shown for Aβ-induced neurotoxicity. Aβ binds to integrins directly (Sabo et al., 1995) and integrins regulate Aβ uptake and its neurotoxic effects (Bi et al., 2002). Treatment of primary cortical neurons with Aβ results in FAK activation (Williamson et al., 2002), and aberrant activation of focal adhesion proteins mediates Aβ–induced neuronal dystrophy (Grace et al., 2002; Williamson et al., 2002). In addition, APP, a potential receptor for Aβ (Lorenzo et al., 2000), is found at focal contacts (Sabo et al., 2001); it colocalizes with β1 integrins in neuronal cells (Yamazaki et al., 1997), and antibody-mediated clustering of APP induces significant loss of dendritic spines (Lefort et al., 2012) and neuronal injury through FAK activation (Xu et al., 2009). We found that clustering of APP was sufficient to induce Glu MTs and both APP and caspase-2 expression were required for the formation of stable Glu MTs by Aβ, suggesting that induction of MT stability by Aβ is initiated by the same APP/caspase-2/RhoA pathway that leads to neurotoxicity by Aβ in neurons (Lefort et al., 2012; Pozueta et al., 2013; Troy et al., 2000). Caspases have been already implicated in the induction of apoptosis, synaptic pruning and inhibition of LTP by Aβ, and caspase activity is modulated by exposures to Aβ (D'Amelio et al., 2011; Hyman, 2011; Jo et al., 2011; Klaiman et al., 2008; Nikolaev et al., 2009; Pozueta et al., 2013; Troy et al., 2000). We found that whereas caspase-2, -3 and to a lesser degree caspase-9 all functioned downstream of Aβ in the induction of MT stability, caspase-6 inhibition resulted in higher levels of stable MTs even in non-stimulated cells. Caspase-6 activation occurs early in AD and whereas both α-tubulin and FAK have been identified as its cytosolic substrates, tau, APP, presenilin-1 and -2 are among its

Journal of Cell Science (2014) 127, 1117–1127 doi:10.1242/jcs.143750

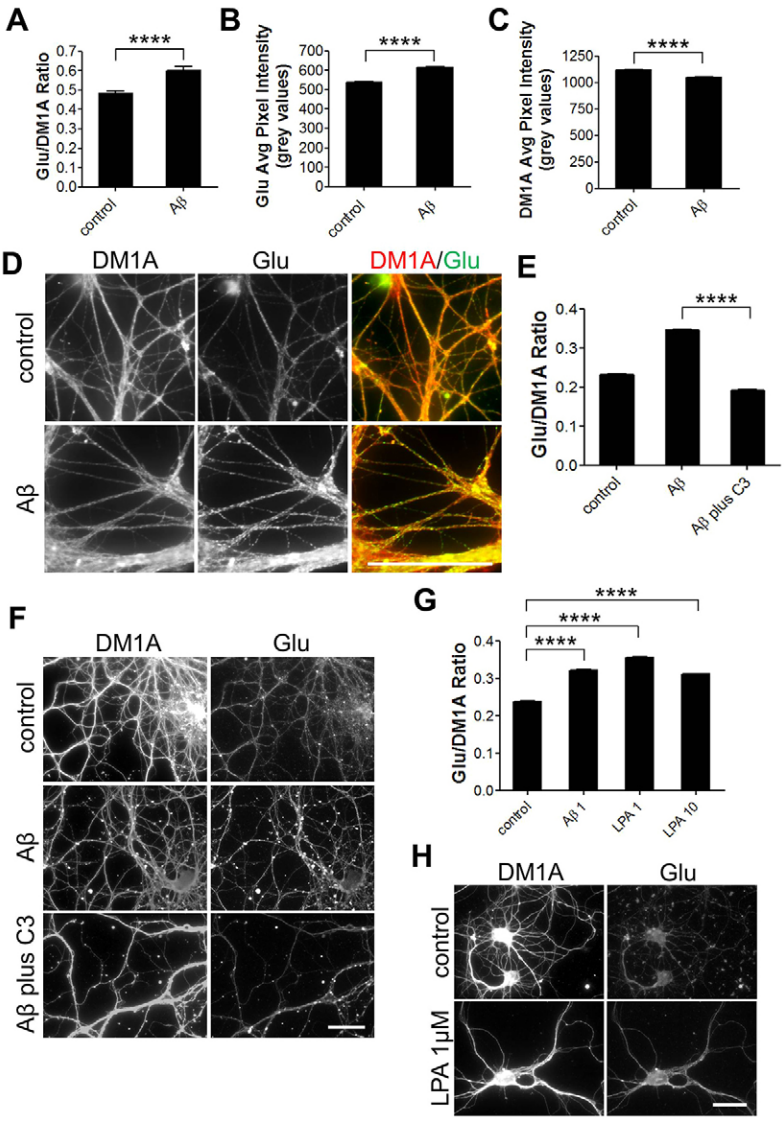

Fig. 6. Aβ induces Glu MTs in cultured rat hippocampal neurons. (A) Quantification of the ratio of measurements for detyrosinated (Glu) to total tubulin (DM1A) in individual neurites of neurons treated with oligomeric $A\beta_{1\text{-}42}$ (0.5 μM) for 3 h. Samples were fixed and processed for immunostaining using specific primary antibodies and Cy-conjugated secondary antibodies. (B) Quantification of detyrosinated tubulin (Glu) levels in neurons treated as in A. (C) Quantification of total tubulin (DM1A) levels in neurons treated as in A. (D) Immunostaining of neurites for detyrosinated tubulin (Glu) and total tubulin (DM1A) in neurons treated as in A. (E) Quantification of the ratio of measurements for detyrosinated (Glu) to total tubulin (DM1A) in individual neurites of neurons incubated with C3 toxin (1.4 μg/ml for 4 h) prior to Aβ (1 μM) for 3 h. (F) Immunostaining of neurites for detyrosinated tubulin (Glu) and total tubulin (DM1A) in neurons treated as in E. (G) Quantification of the ratio of measurements for detyrosinated (Glu) to total tubulin (DM1A) in individual neurites of neurons incubated with LPA (1 and 10 μM) or Aβ (1 μM) for 3 h. (H) Immunostaining of neurites for detyrosinated tubulin (Glu) and total tubulin (DM1A) in neurons treated as in G. ****$P<0.0001$ (Student's *t*-test). Scale bars: 20 μm.

substrates in neurons (Guo et al., 2004; Klaiman et al., 2008; LeBlanc et al., 1999; Pellegrini et al., 1999). Further work will be required to assess whether caspase-6 activity in AD is directly regulated by Aβ or whether it is indirectly activated as a compensatory response to an increase in MT stability. Interestingly, caspase activity is also necessary for induction of Glu MTs by LPA, another potent activator of RhoA, implicating caspases in the regulation of MT dynamics downstream of both physiological and pathological stimuli.

We observed Rho-dependent induction of Glu tubulin levels in neurites of neurons treated with oligomeric Aβ. Neurons have elevated levels of tubulin post-translational modifications that are associated with MT longevity, and analyses of mammalian brain tissue and cultured neuronal cells have shown enrichment of detyrosinated, acetylated, poly-glutamylated and D2-tubulin subunits during differentiation (Janke and Kneussel, 2010). Most of these post-translational modifications have been implicated in the regulation of MAPs, MT-severing enzymes and binding of tubulin to motor proteins (Janke and Bulinski, 2011; Janke and Kneussel, 2010). Synaptic activation also appears to locally regulate MT post-translational modifications that are associated with MT stability (Maas et al., 2009). Thus, localized increases in MT stability in neurons have the potential to (1) impair MT-dependent axonal and dendritic trafficking, (2) directly disrupt synaptic transmission leading to spine collapse, and (3) induce tubulin post-translational modifications that might have deleterious changes in the MT-binding affinity of severing enzymes and MAPs.

We note that our finding that short exposures to Aβ can induce MT stability in neurons challenges the current interpretation that a primary activity of Aβ is to cause MT destabilization through tau hyperphosphorylation (Michaelis et al., 1998) (Ballatore et al., 2012; Michaelis et al., 2005; Zempel et al., 2010; Zhang et al., 2012). We believe that our data, although surprising, are not in contradiction with the current model but rather suggest an original interpretation that deserves further testing, that is that progressive MT destabilization upon exposure to Aβ might be a consequence of the cellular response to counteract a chronic induction in the levels of stable Glu MTs. Interestingly, stable Glu MTs are preferentially depolymerized by tau overexpression in astrocytes (Yoshiyama et al., 2003) and Taxol-induced detyrosination of MTs in tau-depleted neurons restores Aβ-mediated toxicity in these cells (Rapoport et al., 2002). Taken together, these data suggest that stable Glu MTs might contribute

Journal of Cell Science (2014) 127, 1117–1127 doi:10.1242/jcs.143750

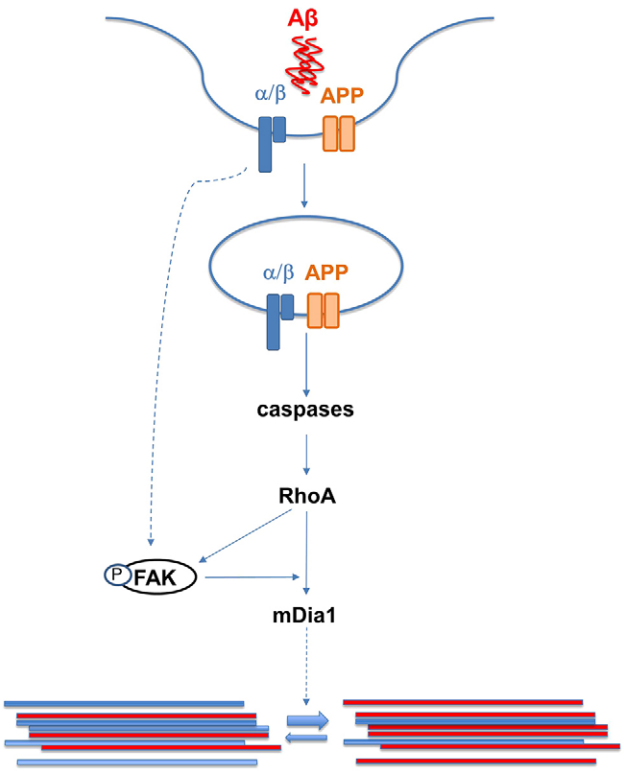

Fig. 7. Proposed model for the pathways involved in Aβ induction of stable detyrosinated MTs. Oligomeric $Aβ_{1-42}$ induces the formation of stable detyrosinated MTs through a pathway regulated by integrin signaling, APP and Rho-mediated activation of mDia1. Signaling of Aβ through APP and integrins at the cell surface or in an endocytic compartment is likely to be the first step in the cascade that leads to RhoA-GTP and mDia1 activation through caspase activity. Active FAK and elevated RhoA-GTP levels are also potentially responsible for further FAK activation, which would then lead to focal adhesion assembly and formation of stable detyrosinated MTs (red bars) from dynamic ones (blue bars) through the action of the formin mDia1.

to tau toxicity by Aβ. If so, synaptic dysfunction, which is believed to be the primary damage caused by Aβ, could result from at least three distinct mechanisms: (1) stabilization of the dynamics of individual MTs in dendritic spines eventually leading to their collapse; (2) indirect stimulation of tau phosphorylation and missorting into a dendritic compartment as a stress-response to a deleterious increase of stable Glu MTs; and (3) tau-dependent or independent recruitment of severing enzymes, such as spastin or katanin, that act more strongly on stable MTs. Surprisingly, whether the behavior of tau protein in AD could be mediated by changes of MT post-translational modifications induced by Aβ has not been explored yet. By contrast, a recent paper suggests that early MT loss by Aβ is caused by tau-mediated TTLL6 mislocalization and poly-glutamylation of dendritic MTs (Zempel et al., 2013). The severing enzyme spastin would then be recruited to MTs through the poly-glutamylation, eventually leading to spine loss, mitochondria and neurofilament mislocalization (Zempel et al., 2013). Interestingly, an opposite role for tau in protecting MTs from being disassembled by katanin, another MT-severing enzyme, has also been shown (Qiang et al., 2006). Thus, at least in the case of poly-glutamylation, tau would be directly responsible for the MT post-translational modification that mediates tau-induced neurotoxicity rather than being affected by it. Induction of Glu MTs by Aβ can occur in the absence of tau expression, yet it remains to be determined whether tau has any role in regulating Glu MT formation by Aβ in neurons. For example, it will be interesting to test whether Glu MTs generated by Aβ can be a preferential target of MT-severing enzymes through a tau-dependent or independent mechanism.

All of the players identified downstream of Aβ in the induction of MT stabilization in NIH3T3 cells are highly conserved, suggesting that the pathways that lead to Glu MT formation are the same in neurons (Fig. 7). However, Aβ can clearly induce Glu MTs independently of tau, therefore opening the door to studying regulation of RhoA/mDia1 activation through integrin-mediated signaling initiated by Aβ not only in neurons but in non-neuronal cells of the central nervous system (CNS) as well. Activated microglia and astrocytes are found in association with amyloid plaques in AD and they could have a role in clearance of the amyloid aggregates as well as in neurotoxicity mediated by Aβ because of the inflammatory reaction they generate. Therefore, whereas, in neurons, our data contribute to the molecular nature of the link between Aβ and tau in causing neurotoxicity in AD, a question that has remained unresolved for decades, the potential involvement of this pathway in astrocytes and/or microglia activation will help us to understand the pathogenic role of these cells in AD. More importantly, should the importance of these findings to AD be confirmed, this work will provide novel targets for the development of new therapeutic strategies to rescue impairment of cell function and cognition in AD.

MATERIALS AND METHODS

Plasmids and reagents

All chemicals were obtained from Sigma-Aldrich (St. Louis, MO), unless otherwise noted. LPA was purchased from Avanti (Alabaster, AL) and C3 TAT from Cytoskeleton Inc (Denver, CO). FAK inhibitor (PF 573228) was from Tocris Bioscience (Ellisville, MO). $Aβ_{1-42}$ was from David Teplow (UCLA, Los Angeles, CA). Caspase inhibitors (pan-caspase, Z-VAD-FMK; caspase-2, Z-VDVAD-FMK; caspase-3, Z-DEVD-FMK; caspase-6, Z-VEID-FMK; and caspase-9, Z-LEHD-FMK) were purchased from Biovision (San Francisco, CA).

Preparation of oligomeric Aβ

Oligomeric $Aβ_{1-42}$ was prepared according to the methods of Stine et al. (Stine et al., 2003). Lyophilized $Aβ_{1-42}$ was allowed to equilibrate to room tempearture for 30 min to avoid condensation upon opening the vial. The lyophilized peptide was resuspended in 1,1,1,3,3,3-hexafluoro-2-propanol (HFIP) to a concentration of 1 mM using a gas-tight Hamilton syringe with a Teflon plunger. HFIP was allowed to evaporate in a fume hood overnight. The resulting clear film was dried under vacuum (6.7 mTorr) in a SpeedVac and the dessicated pellet was stored at −20℃. Immediately prior to use, the aliquots were resuspended to a concentration of 5 mM in DMSO by pipette mixing followed by bath sonication for 10 min at 4℃. The resuspended peptide was diluted to 100 µM in ice-cold HAM F12 medium, immediately vortexed for 30 s and incubated at 4℃ for 24 h. The concentration of Aβ was determined based on the amounts of total Aβ content in our preparation including different forms of oligomeric Aβ.

Antibodies

Primary antibodies used for western blotting (WB) or immunofluorescence (IF) were: rabbit anti-detyrosinated tubulin (SG, 1:10,000 WB, 1:500 IF), mouse anti-total tubulin (DM1A, 1:100 IF), rat anti-tyrosinated tubulin (YL1/2, 1:10 IF), mouse anti-acetylated tubulin (6-11-B1, 1:10,000 WB, 1:100 IF), mouse anti-GAPDH (1:8000), rabbit anti-RhoA (67B9, Cell Signaling, 1:1000 WB), mouse anti-p^{Y397}FAK (1:1000 WB, 1:50 IF, BD Transduction), rabbit anti-p^{Y577}FAK (rabbit, 1:50 IF, Invitrogen), rabbit anti-FAK (C-20, Santa Cruz, 1:500 WB),

mouse anti-APP (22C11, Millipore, 1:100 WB), mouse anti-pericentrin (1:100 IF, BD Transduction), rabbit anti-pMyosin light-chain (1:200 IF, Cell Signaling) and mouse anti-vinculin (1:100 IF). For western blot analysis, secondary antibodies were conjugated to IR680 or IR800 (Rockland Immunochemicals) for multiple infrared detection. For immunofluorescence analysis, primary antibodies incubation was followed by use of the appropriate Cy-dye-conjugated secondary antibodies pre-absorbed to minimize cross-reaction (Jackson Immunoresearch Laboratories).

Cell cultures and incubation with drugs or antibodies

NIH3T3 cells were grown in DMEM and 10% calf serum, whereas $FAK^{-/-}$ cells (Ilić et al., 1995) were grown in DMEM plus 10% fetal calf serum, as previously described (Cook et al., 1998; Kreitzer et al., 1999; Palazzo et al., 2001a). For Aβ and LPA incubations or drug inhibition experiments, cells were grown to confluence on acid-washed coverslips and serum-starved for 48 h to downregulate MT stabilization. Confluent monolayers were wounded 30 min before drug, LPA or Aβ addition. In the case of C3 TAT inhibition, the drug was added 4 h prior to Aβ incubation at 2 µg/ml, whereas FAK inhibitor was added at 10 µM at 1 h prior to addition of Aβ. Z-VAD-FMK and all specific caspase inhibitors were added at 10 µM 1 h prior to Aβ treatment. The 22C11 APP antibody (Millipore, MA) and its Fab fragment (Lefort et al., 2012) were added to starved cells for 4 h at the indicated final concentrations. Primary cultures of hippocampal neurons were generated from fetuses at embryonic day 18 (E18) from timed pregnant Sprague-Dawley rats (Taconic Farms) that were killed prior to hippocampi removal. Neurons were then dissociated, plated at a density of 2×10^5 cells/ml on plates coated with poly-L-lysine and maintained in a defined serum-free medium (95% neurobasal, 2% B-27 supplement, 0.5 mM L-glutamine, 0.6% glucose). Cultures at 10–21 days *in vitro* (DIV) were used for the experiments. All animal experiments were performed according to approved guidelines.

Cell spreading assays

Cell spreading assays were carried out as previously described (Palazzo et al., 2004). Briefly, NIH3T3 cells grown in serum-containing medium were detached with trypsin, the trypsin was quenched with soybean trypsin inhibitor (1 mg/ml in PBS), and the cells collected by gentle centrifugation. After washing twice with DMEM plus 2% BSA, cells were incubated at 37℃ for 60 min with regular rotation to prevent cell clumping. Cells were then allowed to attach on coverslips coated with poly-lysine (100 µg/ml in PBS) or fibronectin (100 µg/ml in PBS) for the indicated times in the presence of Aβ or LPA at the indicated concentrations prior to methanol fixation for 10 min at −20℃.

siRNA transfection and western blot analysis

NIH3T3 cells were transfected with siRNA oligonucelotides (Shangai GenePharma) using RNAiMax according to the manufacturer's specifications (Invitrogen). siRNA duplexes targeting mDia1, and caspase-2 and -3 were based on previously published sequences (Ahmed et al., 2011; Eng et al., 2006; Wurzer et al., 2003). APP1 (5′-GGGAAGAGGCAGAGCGTCA-3′) and APP2 (5′- CGGAAGAGATC-TCGGAAGT-3′), used to silence APP, were generated through the Dharmacon siRNA design algorithm (http://www.thermoscientificbio.com/design-center/). A scrambled non-coding sequence (NC) provided by the manufacturer was used as a negative control. siRNA oligoduplexes were all resuspended in RNase-free water and stored at a concentration of 20 µM. Knocked-down efficiency and effects on Glu MTs were typically analyzed 96 h after transfection and 48 h after serum-starvation. For western blot analysis, cells were lysed in RIPA buffer (1% Triton X-100, 50 mM Tris-HCl pH 7.4, 150 mM NaCl, 0.1% SDS, 0.5% Na-deoxycholate, 1 mM phenylmethylsulfonyl fluoride, and protease and phosphatase inhibitors mix from Pierce), normalized for loading by bicinchonic acid assay before boiling in Laemmli sample buffer and protein separation by SDS-PAGE. Image acquisition was performed with an Odyssey imaging system (LI-COR Biosciences, NE) and images digitally processed with Adobe Photoshop (San Jose, CA).

RhoA-GTP pull-down assays

RhoA-GTP pull-down assays were performed following the manufacturer's protocol (Cytoskeleton, Inc.). Briefly, cells were washed once with ice-cold PBS and lysed with RIPA and M-PER buffer (1:1; Thermo Scientific). Lysates were briefly vortexed, incubated on ice for 5 min, centrifuged (10,000 ***g***) for 5 min and divided into two samples: one for input and the remaining for pull-down. To pull-down active RhoA, lysates were incubated by rotating for 1 h at 4℃ with Rhotekin-RBD protein beads (25 µl). Beads were collected by centrifugation at 4℃ and washed 2× with 500 µl ice-cold lysis buffer. Beads and input samples were then analyzed by western blotting using a RhoA-specific antibody.

Epifluorescence microscopy

In most immunostaining experiments, cells were fixed in methanol at −20℃ for 10 min (5 min for neurons) and rehydrated in 10 mM Tris-buffered saline (TBS), pH 7.4. Cells were stained by double indirect immunofluorescence, using specific primary antibodies. For quantification of F-actin levels, cells were fixed in 4% paraformaldehyde for 15 min and then briefly permeabilized in Triton X-100 0.5% prior to staining using Rhodamine–phalloidin (Invitrogen, 1:200). Mounted samples were observed by epifluorescence microscope (Nikon Optiphot) using a 60× Plan-Apochromat objective and filter cubes optimized for coumarin, fluorescin and GFP, Rhodamine and Cy5 fluorescence. Still images were acquired with a MicroMax camera (Kodak KAF 1440-chip; Princeton Instruments, NJ) using MetaMorph software (MDS Analytical Technologies, Sunnyvale, CA). For each condition, stable Glu MTs were counted in 200 cells at the edge of an artificial wound and quantified by scoring the percentage of cells with at least ten brightly stained detyrosinated (Glu) MTs. This cut-off was chosen because previous data have shown that serum-starved NIH3T3 cells have less than ten Glu MTs (Cook et al., 1998; Gundersen et al., 1994; Palazzo et al., 2001a). Scoring was performed blinded and results quantified and expressed as the means±s.e.m. from at least three independent experiments.

Imaging analysis

To quantify cellular F-actin staining, one region was drawn around the perimeter of each cell (30 cells per condition) and gray intensity average values measured by Metamorph software after background subtraction. To quantify focal adhesions (FAs), we used the 'thresholding' function to create a binary image identifying all FAs in each image. The 'analyze particles' function was then applied to calculate their number and intensity. For measuring the intensity of Glu and DM1A staining in neurons, lines were drawn on individual neurites using the 'traced line' tool in the Metamorph software, and the average pixel intensities of both signals were measured on that line. A total of 3300 pixels were recorded per data point per experiment and their means analyzed for statistical significance.

Statistics

Experiments were performed blinded and results are expressed as the means±s.e.m.. In all cases, the level of significance is set at $P<0.05$. Statistical analysis of non-parametric data, such as scoring of Glu MTs, MTOC reorientation or dead cells in cytotoxicity assays was carried out using a Chi square test. For Rho-GTP pull-down experiments, F-actin, focal adhesion number and intensity measurements and for measurements of Glu and DM1A levels in neurons, raw data were analyzed using Prism 4 (GraphPad Software, Inc.) by a two-tailed unpaired Student's *t*-test.

Cell permeabilization assays

Serum-starved NIH3T3 were wounded and treated with Aβ for 1 h prior to addition of nocodazole for an additional 1 h at 2 µM. At the end of the incubation time, cells were gently rinsed in warm microtubule stabilization buffer (MSB) (85 mM PIPES pH 6.9, 1 mM EGTA, 1 mM $MgCl_2$, 2 M glycerol and protease inhibitors mix from Pierce) prior to extraction with MSB supplemented with saponin (200 µg/ml) for 3 min before methanol fixation at −20℃.

MTOC reorientation

For MTOC orientation data, cells were scored as previously described (Palazzo et al., 2001b). Scoring was performed blinded and results quantified and expressed as the means±s.e.m. from at least three independent experiments (n>200 cells per experiment).

Cytotoxicity assays

Cytoxicity assays were performed as described by the manufacturer (L3224, Molecular Probes). Briefly, cells were serum-starved for 48 h and then treated with vehicle or Aβ (1 μM) for 24 h prior to incubation with a freshly made working solution of ethidium homodimer-1 (EthD-1) (4 μM) and calcein (2 μM) at R.T. for 30 min. Following incubation, cells were fixed in paraformaldehyde 4% for 10 min at R.T. and coverslips mounted on slides for viewing under the fluorescence microscope. A total of 200 cells were scored per condition and the percentage of dead cells calculated based on the number of cells with intense fluorescence at >600 nm.

Acknowledgements

The authors are grateful to Sara Nik for excellent technical assistance, Wakam Chang (all Columbia University, NY) for advice on imaging quantification and Jeremy Lai Jun Hei for data analysis. We thank Michael Shelanski and Gregg Gundersen (Columbia University, NY) for very helpful discussions of the data and critical reading of the manuscript.

Competing interests

The authors declare no competing interests.

Author contributions

B.P. performed and analyzed most of the experiments in the manuscript. R.L. contributed to the conception, assays performance, data analysis and writing of the manuscript. L.T. and E.T contributed to data acquisition and analysis. F.B. designed all the experiments, contributed to all data acquisition and analysis, and wrote the manuscript.

Funding

This work was supported by a New Investigator Research Grant from the Alzheimer's Association [grant number NIRP-12-259038 to F.B.].

Supplementary material

Supplementary material available online at
http://jcs.biologists.org/lookup/suppl/doi:10.1242/jcs.143750/-/DC1

References

Ahmed, Z., Kalinski, H., Berry, M., Almasieh, M., Ashush, H., Slager, N., Brafman, A., Spivak, I., Prasad, N., Mett, I. et al. (2011). Ocular neuroprotection by siRNA targeting caspase-2. *Cell Death Dis.* **2**, e173.

Andrés-Delgado, L., Antón, O. M., Bartolini, F., Ruiz-Sáenz, A., Correas, I., Gundersen, G. G. and Alonso, M. A. (2012). INF2 promotes the formation of detyrosinated microtubules necessary for centrosome reorientation in T cells. *J. Cell Biol.* **198**, 1025-1037.

Ballatore, C., Brunden, K. R., Huryn, D. M., Trojanowski, J. Q., Lee, V. M. and Smith, A. B., 3rd (2012). Microtubule stabilizing agents as potential treatment for Alzheimer's disease and related neurodegenerative tauopathies. *J. Med. Chem.* **55**, 8979-8996.

Bartolini, F. and Gundersen, G. G. (2010). Formins and microtubules. *Biochim. Biophys. Acta* **1803**, 164-173.

Bartolini, F., Moseley, J. B., Schmoranzer, J., Cassimeris, L., Goode, B. L. and Gundersen, G. G. (2008). The formin mDia2 stabilizes microtubules independently of its actin nucleation activity. *J. Cell Biol.* **181**, 523-536.

Bartolini, F., Ramalingam, N. and Gundersen, G. G. (2012). Actin-capping protein promotes microtubule stability by antagonizing the actin activity of mDia1. *Mol. Biol. Cell* **23**, 4032-4040.

Bi, X., Gall, C. M., Zhou, J. and Lynch, G. (2002). Uptake and pathogenic effects of amyloid beta peptide 1-42 are enhanced by integrin antagonists and blocked by NMDA receptor antagonists. *Neuroscience* **112**, 827-840.

Borysov, S. I., Granic, A., Padmanabhan, J., Walczak, C. E. and Potter, H. (2011). Alzheimer Aβ disrupts the mitotic spindle and directly inhibits mitotic microtubule motors. *Cell Cycle* **10**, 1397-1410.

Busciglio, J., Lorenzo, A., Yeh, J. and Yankner, B. A. (1995). beta-amyloid fibrils induce tau phosphorylation and loss of microtubule binding. *Neuron* **14**, 879-888.

Chacon, P. J., Garcia-Mejias, R. and Rodriguez-Tebar, A. (2011). Inhibition of RhoA GTPase and the subsequent activation of PTP1B protects cultured hippocampal neurons against amyloid β toxicity. *Mol. Neurodegener.* **6**, 14.

Chesarone, M. A., DuPage, A. G. and Goode, B. L. (2010). Unleashing formins to remodel the actin and microtubule cytoskeletons. *Nat. Rev. Mol. Cell Biol.* **11**, 62-74.

Chrzanowska-Wodnicka, M. and Burridge, K. (1996). Rho-stimulated contractility drives the formation of stress fibers and focal adhesions. *J. Cell Biol.* **133**, 1403-1415.

Cook, T. A., Nagasaki, T. and Gundersen, G. G. (1998). Rho guanosine triphosphatase mediates the selective stabilization of microtubules induced by lysophosphatidic acid. *J. Cell Biol.* **141**, 175-185.

D'Amelio, M., Cavallucci, V., Middei, S., Marchetti, C., Pacioni, S., Ferri, A., Diamantini, A., De Zio, D., Carrara, P., Battistini, L. et al. (2011). Caspase-3 triggers early synaptic dysfunction in a mouse model of Alzheimer's disease. *Nat. Neurosci.* **14**, 69-76.

Dunn, S., Morrison, E. E., Liverpool, T. B., Molina-París, C., Cross, R. A., Alonso, M. C. and Peckham, M. (2008). Differential trafficking of Kif5c on tyrosinated and detyrosinated microtubules in live cells. *J. Cell Sci.* **121**, 1085-1095.

Eng, C. H., Huckaba, T. M. and Gundersen, G. G. (2006). The formin mDia regulates GSK3beta through novel PKCs to promote microtubule stabilization but not MTOC reorientation in migrating fibroblasts. *Mol. Biol. Cell* **17**, 5004-5016.

Ferreira, A., Lu, Q., Orecchio, L. and Kosik, K. S. (1997). Selective phosphorylation of adult tau isoforms in mature hippocampal neurons exposed to fibrillar A beta. *Mol. Cell. Neurosci.* **9**, 220-234.

Gomes, E. R., Jani, S. and Gundersen, G. G. (2005). Nuclear movement regulated by Cdc42, MRCK, myosin, and actin flow establishes MTOC polarization in migrating cells. *Cell* **121**, 451-463.

Goulimari, P., Kitzing, T. M., Knieling, H., Brandt, D. T., Offermanns, S. and Grosse, R. (2005). Galpha12/13 is essential for directed cell migration and localized Rho-Dia1 function. *J. Biol. Chem.* **280**, 42242-42251.

Goulimari, P., Knieling, H., Engel, U. and Grosse, R. (2008). LARG and mDia1 link Galpha12/13 to cell polarity and microtubule dynamics. *Mol. Biol. Cell* **19**, 30-40.

Grace, E. A., Rabiner, C. A. and Busciglio, J. (2002). Characterization of neuronal dystrophy induced by fibrillar amyloid beta: implications for Alzheimer's disease. *Neuroscience* **114**, 265-273.

Gundersen, G. G., Kalnoski, M. H. and Bulinski, J. C. (1984). Distinct populations of microtubules: tyrosinated and nontyrosinated alpha tubulin are distributed differently in vivo. *Cell* **38**, 779-789.

Gundersen, G. G., Kim, I. and Chapin, C. J. (1994). Induction of stable microtubules in 3T3 fibroblasts by TGF-beta and serum. *J. Cell Sci.* **107**, 645-659.

Guo, H., Albrecht, S., Bourdeau, M., Petzke, T., Bergeron, C. and LeBlanc, A. C. (2004). Active caspase-6 and caspase-6-cleaved tau in neuropil threads, neuritic plaques, and neurofibrillary tangles of Alzheimer's disease. *Am. J. Pathol.* **165**, 523-531.

Hallak, M. E., Rodriguez, J. A., Barra, H. S. and Caputto, R. (1977). Release of tyrosine from tyrosinated tubulin. Some common factors that affect this process and the assembly of tubulin. *FEBS Lett.* **73**, 147-150.

Hernandez, F., Lucas, J. J. and Avila, J. (2013). GSK3 and tau: two convergence points in Alzheimer's disease. *J. Alzheimers Dis.* **33 Suppl. 1**, S141-S144.

Hyman, B. T. (2011). Caspase activation without apoptosis: insight into Aβ initiation of neurodegeneration. *Nat. Neurosci.* **14**, 5-6.

Ilić, D., Furuta, Y., Kanazawa, S., Takeda, N., Sobue, K., Nakatsuji, N., Nomura, S., Fujimoto, J., Okada, M. and Yamamoto, T. (1995). Reduced cell motility and enhanced focal adhesion contact formation in cells from FAK-deficient mice. *Nature* **377**, 539-544.

Ittner, L. M. and Götz, J. (2011). Amyloid-β and tau – a toxic pas de deux in Alzheimer's disease. *Nat. Rev. Neurosci.* **12**, 65-72.

Janke, C. and Bulinski, J. C. (2011). Post-translational regulation of the microtubule cytoskeleton: mechanisms and functions. *Nat. Rev. Mol. Cell Biol.* **12**, 773-786.

Janke, C. and Kneussel, M. (2010). Tubulin post-translational modifications: encoding functions on the neuronal microtubule cytoskeleton. *Trends Neurosci.* **33**, 362-372.

Jo, J., Whitcomb, D. J., Olsen, K. M., Kerrigan, T. L., Lo, S. C., Bru-Mercier, G., Dickinson, B., Scullion, S., Sheng, M., Collingridge, G. et al. (2011). Aβ(1-42) inhibition of LTP is mediated by a signaling pathway involving caspase-3, Akt1 and GSK-3β. *Nat. Neurosci.* **14**, 545-547.

King, M. E., Kan, H. M., Baas, P. W., Erisir, A., Glabe, C. G. and Bloom, G. S. (2006). Tau-dependent microtubule disassembly initiated by prefibrillar beta-amyloid. *J. Cell Biol.* **175**, 541-546.

Klaiman, G., Petzke, T. L., Hammond, J. and Leblanc, A. C. (2008). Targets of caspase-6 activity in human neurons and Alzheimer disease. *Mol. Cell. Proteomics* **7**, 1541-1555.

Konishi, Y. and Setou, M. (2009). Tubulin tyrosination navigates the kinesin-1 motor domain to axons. *Nat. Neurosci.* **12**, 559-567.

Kreitzer, G., Liao, G. and Gundersen, G. G. (1999). Detyrosination of tubulin regulates the interaction of intermediate filaments with microtubules in vivo via a kinesin-dependent mechanism. *Mol. Biol. Cell* **10**, 1105-1118.

LaFerla, F. M. (2010). Pathways linking Abeta and tau pathologies. *Biochem. Soc. Trans.* **38**, 993-995.

Lambert, M. P., Barlow, A. K., Chromy, B. A., Edwards, C., Freed, R., Liosatos, M., Morgan, T. E., Rozovsky, I., Trommer, B., Viola, K. L. et al. (1998). Diffusible, nonfibrillar ligands derived from Abeta1-42 are potent central nervous system neurotoxins. *Proc. Natl. Acad. Sci. USA* **95**, 6448-6453.

LeBlanc, A., Liu, H., Goodyer, C., Bergeron, C. and Hammond, J. (1999). Caspase-6 role in apoptosis of human neurons, amyloidogenesis, and Alzheimer's disease. *J. Biol. Chem.* **274**, 23426-23436.

Lefort, R., Pozueta, J. and Shelanski, M. (2012). Cross-linking of cell surface amyloid precursor protein leads to increased β-amyloid peptide production in

hippocampal neurons: implications for Alzheimer's disease. *J. Neurosci.* **32**, 10674-10685.

Lesné, S., Koh, M. T., Kotilinek, L., Kayed, R., Glabe, C. G., Yang, A., Gallagher, M. and Ashe, K. H. (2006). A specific amyloid-beta protein assembly in the brain impairs memory. *Nature* **440**, 352-357.

Liao, G., Kreitzer, G., Cook, T. A. and Gundersen, G. G. (1999). A signal transduction pathway involved in microtubule-mediated cell polarization. *FASEB J.* **13 Suppl. 2**, S257-S260.

Lorenzo, A., Yuan, M., Zhang, Z., Paganetti, P. A., Sturchler-Pierrat, C., Staufenbiel, M., Mautino, J., Vigo, F. S., Sommer, B. and Yankner, B. A. (2000). Amyloid beta interacts with the amyloid precursor protein: a potential toxic mechanism in Alzheimer's disease. *Nat. Neurosci.* **3**, 460-464.

Maas, C., Belgardt, D., Lee, H. K., Heisler, F. F., Lappe-Siefke, C., Magiera, M. M., van Dijk, J., Hausrat, T. J., Janke, C. and Kneussel, M. (2009). Synaptic activation modifies microtubules underlying transport of postsynaptic cargo. *Proc. Natl. Acad. Sci. USA* **106**, 8731-8736.

Michaelis, M. L., Ranciat, N., Chen, Y., Bechtel, M., Ragan, R., Hepperle, M., Liu, Y. and Georg, G. (1998). Protection against beta-amyloid toxicity in primary neurons by paclitaxel (Taxol). *J. Neurochem.* **70**, 1623-1627.

Michaelis, M. L., Ansar, S., Chen, Y., Reiff, E. R., Seyb, K. I., Himes, R. H., Audus, K. L. and Georg, G. I. (2005). beta-Amyloid-induced neurodegeneration and protection by structurally diverse microtubule-stabilizing agents. *J. Pharmacol. Exp. Ther.* **312**, 659-668.

Nagasaki, T. and Gundersen, G. G. (1996). Depletion of lysophosphatidic acid triggers a loss of oriented detyrosinated microtubules in motile fibroblasts. *J. Cell Sci.* **109**, 2461-2469.

Nikolaev, A., McLaughlin, T., O'Leary, D. D. and Tessier-Lavigne, M. (2009). APP binds DR6 to trigger axon pruning and neuron death via distinct caspases. *Nature* **457**, 981-989.

Nimmrich, V. and Ebert, U. (2009). Is Alzheimer's disease a result of presynaptic failure? Synaptic dysfunctions induced by oligomeric beta-amyloid. *Rev. Neurosci.* **20**, 1-12.

Palazzo, A. F., Cook, T. A., Alberts, A. S. and Gundersen, G. G. (2001a). mDia mediates Rho-regulated formation and orientation of stable microtubules. *Nat. Cell Biol.* **3**, 723-729.

Palazzo, A. F., Joseph, H. L., Chen, Y. J., Dujardin, D. L., Alberts, A. S., Pfister, K. K., Vallee, R. B. and Gundersen, G. G. (2001b). Cdc42, dynein, and dynactin regulate MTOC reorientation independent of Rho-regulated microtubule stabilization. *Curr. Biol.* **11**, 1536-1541.

Palazzo, A. F., Eng, C. H., Schlaepfer, D. D., Marcantonio, E. E. and Gundersen, G. G. (2004). Localized stabilization of microtubules by integrin- and FAK-facilitated Rho signaling. *Science* **303**, 836-839.

Pellegrini, L., Passer, B. J., Tabaton, M., Ganjei, J. K. and D'Adamio, L. (1999). Alternative, non-secretase processing of Alzheimer's beta-amyloid precursor protein during apoptosis by caspase-6 and -8. *J. Biol. Chem.* **274**, 21011-21016.

Peris, L., Thery, M., Fauré, J., Saoudi, Y., Lafanechère, L., Chilton, J. K., Gordon-Weeks, P., Galjart, N., Bornens, M., Wordeman, L. et al. (2006). Tubulin tyrosination is a major factor affecting the recruitment of CAP-Gly proteins at microtubule plus ends. *J. Cell Biol.* **174**, 839-849.

Peris, L., Wagenbach, M., Lafanechère, L., Brocard, J., Moore, A. T., Kozielski, F., Job, D., Wordeman, L. and Andrieux, A. (2009). Motor-dependent microtubule disassembly driven by tubulin tyrosination. *J. Cell Biol.* **185**, 1159-1166.

Petratos, S., Li, Q. X., George, A. J., Hou, X., Kerr, M. L., Unabia, S. E., Hatzinisiriou, I., Maksel, D., Aguilar, M. I. and Small, D. H. (2008). The beta-amyloid protein of Alzheimer's disease increases neuronal CRMP-2 phosphorylation by a Rho-GTP mechanism. *Brain* **131**, 90-108.

Playford, M. P. and Schaller, M. D. (2004). The interplay between Src and integrins in normal and tumor biology. *Oncogene* **23**, 7928-7946.

Pozueta, J., Lefort, R., Ribe, E. M., Troy, C. M., Arancio, O. and Shelanski, M. (2013). Caspase-2 is required for dendritic spine and behavioural alterations in J20 APP transgenic mice. *Nat. Commun.* **4**, 1939.

Qiang, L., Yu, W., Andreadis, A., Luo, M. and Baas, P. W. (2006). Tau protects microtubules in the axon from severing by katanin. *J. Neurosci.* **26**, 3120-3129.

Rapoport, M., Dawson, H. N., Binder, L. I., Vitek, M. P. and Ferreira, A. (2002). Tau is essential to beta -amyloid-induced neurotoxicity. *Proc. Natl. Acad. Sci. USA* **99**, 6364-6369.

Rohn, T. T., Ivins, K. J., Bahr, B. A., Cotman, C. W. and Cribbs, D. H. (2000). A monoclonal antibody to amyloid precursor protein induces neuronal apoptosis. *J. Neurochem.* **74**, 2331-2342.

Sabo, S., Lambert, M. P., Kessey, K., Wade, W., Krafft, G. and Klein, W. L. (1995). Interaction of beta-amyloid peptides with integrins in a human nerve cell line. *Neurosci. Lett.* **184**, 25-28.

Sabo, S. L., Ikin, A. F., Buxbaum, J. D. and Greengard, P. (2001). The Alzheimer amyloid precursor protein (APP) and FE65, an APP-binding protein, regulate cell movement. *J. Cell Biol.* **153**, 1403-1414.

Schulze, E. and Kirschner, M. (1987). Dynamic and stable populations of microtubules in cells. *J. Cell Biol.* **104**, 277-288.

Schulze, E., Asai, D. J., Bulinski, J. C. and Kirschner, M. (1987). Posttranslational modification and microtubule stability. *J. Cell Biol.* **105**, 2167-2177.

Shankar, G. M., Bloodgood, B. L., Townsend, M., Walsh, D. M., Selkoe, D. J. and Sabatini, B. L. (2007). Natural oligomers of the Alzheimer amyloid-beta protein induce reversible synapse loss by modulating an NMDA-type glutamate receptor-dependent signaling pathway. *J. Neurosci.* **27**, 2866-2875.

Stine, W. B., Jr, Dahlgren, K. N., Krafft, G. A. and LaDu, M. J. (2003). In vitro characterization of conditions for amyloid-beta peptide oligomerization and fibrillogenesis. *J. Biol. Chem.* **278**, 11612-11622.

Takashima, A., Noguchi, K., Sato, K., Hoshino, T. and Imahori, K. (1993). Tau protein kinase I is essential for amyloid beta-protein-induced neurotoxicity. *Proc. Natl. Acad. Sci. USA* **90**, 7789-7793.

Takashima, A., Yamaguchi, H., Noguchi, K., Michel, G., Ishiguro, K., Sato, K., Hoshino, T., Hoshi, M. and Imahori, K. (1995). Amyloid beta peptide induces cytoplasmic accumulation of amyloid protein precursor via tau protein kinase I/glycogen synthase kinase-3 beta in rat hippocampal neurons. *Neurosci. Lett.* **198**, 83-86.

Takashima, A., Noguchi, K., Michel, G., Mercken, M., Hoshi, M., Ishiguro, K. and Imahori, K. (1996). Exposure of rat hippocampal neurons to amyloid beta peptide (25-35) induces the inactivation of phosphatidyl inositol-3 kinase and the activation of tau protein kinase I/glycogen synthase kinase-3 beta. *Neurosci. Lett.* **203**, 33-36.

Troy, C. M., Rabacchi, S. A., Friedman, W. J., Frappier, T. F., Brown, K. and Shelanski, M. L. (2000). Caspase-2 mediates neuronal cell death induced by beta-amyloid. *J. Neurosci.* **20**, 1386-1392.

Wen, Y., Eng, C. H., Schmoranzer, J., Cabrera-Poch, N., Morris, E. J., Chen, M., Wallar, B. J., Alberts, A. S. and Gundersen, G. G. (2004). EB1 and APC bind to mDia to stabilize microtubules downstream of Rho and promote cell migration. *Nat. Cell Biol.* **6**, 820-830.

Williamson, R., Scales, T., Clark, B. R., Gibb, G., Reynolds, C. H., Kellie, S., Bird, I. N., Varndell, I. M., Sheppard, P. W., Everall, I. et al. (2002). Rapid tyrosine phosphorylation of neuronal proteins including tau and focal adhesion kinase in response to amyloid-beta peptide exposure: involvement of Src family protein kinases. *J. Neurosci.* **22**, 10-20.

Wurzer, W. J., Planz, O., Ehrhardt, C., Giner, M., Silberzahn, T., Pleschka, S. and Ludwig, S. (2003). Caspase 3 activation is essential for efficient influenza virus propagation. *EMBO J.* **22**, 2717-2728.

Xu, Y. X., Wang, H. Q., Yan, J., Sun, X. B., Guo, J. C. and Zhu, C. Q. (2009). Antibody binding to cell surface amyloid precursor protein induces neuronal injury by deregulating the phosphorylation of focal adhesion signaling related proteins. *Neurosci. Lett.* **465**, 276-281.

Yamazaki, T., Koo, E. H. and Selkoe, D. J. (1997). Cell surface amyloid beta-protein precursor colocalizes with beta 1 integrins at substrate contact sites in neural cells. *J. Neurosci.* **17**, 1004-1010.

Yoshiyama, Y., Zhang, B., Bruce, J., Trojanowski, J. Q. and Lee, V. M. (2003). Reduction of detyrosinated microtubules and Golgi fragmentation are linked to tau-induced degeneration in astrocytes. *J. Neurosci.* **23**, 10662-10671.

Zempel, H., Thies, E., Mandelkow, E. and Mandelkow, E. M. (2010). Abeta oligomers cause localized Ca(2+) elevation, missorting of endogenous Tau into dendrites, Tau phosphorylation, and destruction of microtubules and spines. *J. Neurosci.* **30**, 11938-11950.

Zempel, H., Luedtke, J., Kumar, Y., Biernat, J., Dawson, H., Mandelkow, E. and Mandelkow, E. M. (2013). Amyloid-β oligomers induce synaptic damage via Tau-dependent microtubule severing by TTLL6 and spastin. *EMBO J.* **32**, 2920-2937.

Zhang, B., Carroll, J., Trojanowski, J. Q., Yao, Y., Iba, M., Potuzak, J. S., Hogan, A. M., Xie, S. X., Ballatore, C., Smith, A. B., III ET AL. (2012). The microtubule-stabilizing agent, epothilone D, reduces axonal dysfunction, neurotoxicity, cognitive deficits, and Alzheimer-like pathology in an interventional study with aged tau transgenic mice. *J. Neurosci.* **32**, 3601-3611.

Zheng, W. H., Bastianetto, S., Mennicken, F., Ma, W. and Kar, S. (2002). Amyloid beta peptide induces tau phosphorylation and loss of cholinergic neurons in rat primary septal cultures. *Neuroscience* **115**, 201-211.

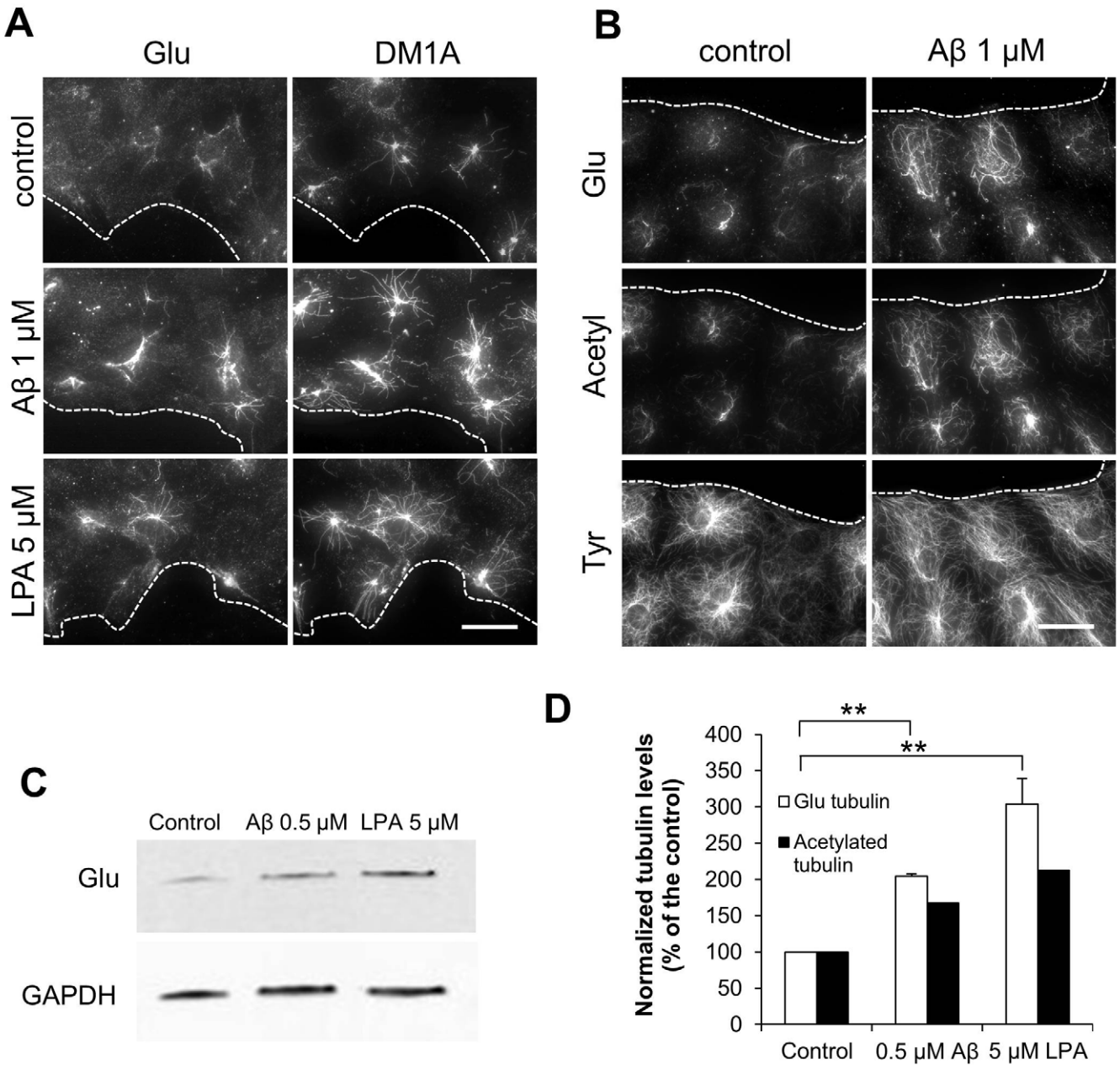

Fig. S1. Glu MTs induced by Aβ are stable. (A) Immunostaining of detyrosinated (Glu) and pan-tubulin (DM1A) in serum-starved cells at the wound treated with Aβ (2 h) and Nocodazole (1 h) prior to brief permeabilization with saponin before fixation. (B) Immunostaining of detyrosinated (Glu), tyrosinated (Tyr) and acetylated (Acetyl) tubulin in cells at the wound treated with Aβ for 2 h. (C) Western blot analysis of whole cell lysates from serum-starved NIH3T3 cells treated with Aβ or LPA prior to harvesting. Detyrosinated tubulin was detected by the Glu antibody and an antibody specific for GAPDH was used as a loading marker. (D) Quantification of the levels of detyrosinated (Glu) or acetylated tubulin normalized against GAPDH levels. In the case of detyrosinated tubulin, the data are mean $\pm$ SEM from three independent experiments. ** $p<0.01$ by t-test. Bars, 20 mm.

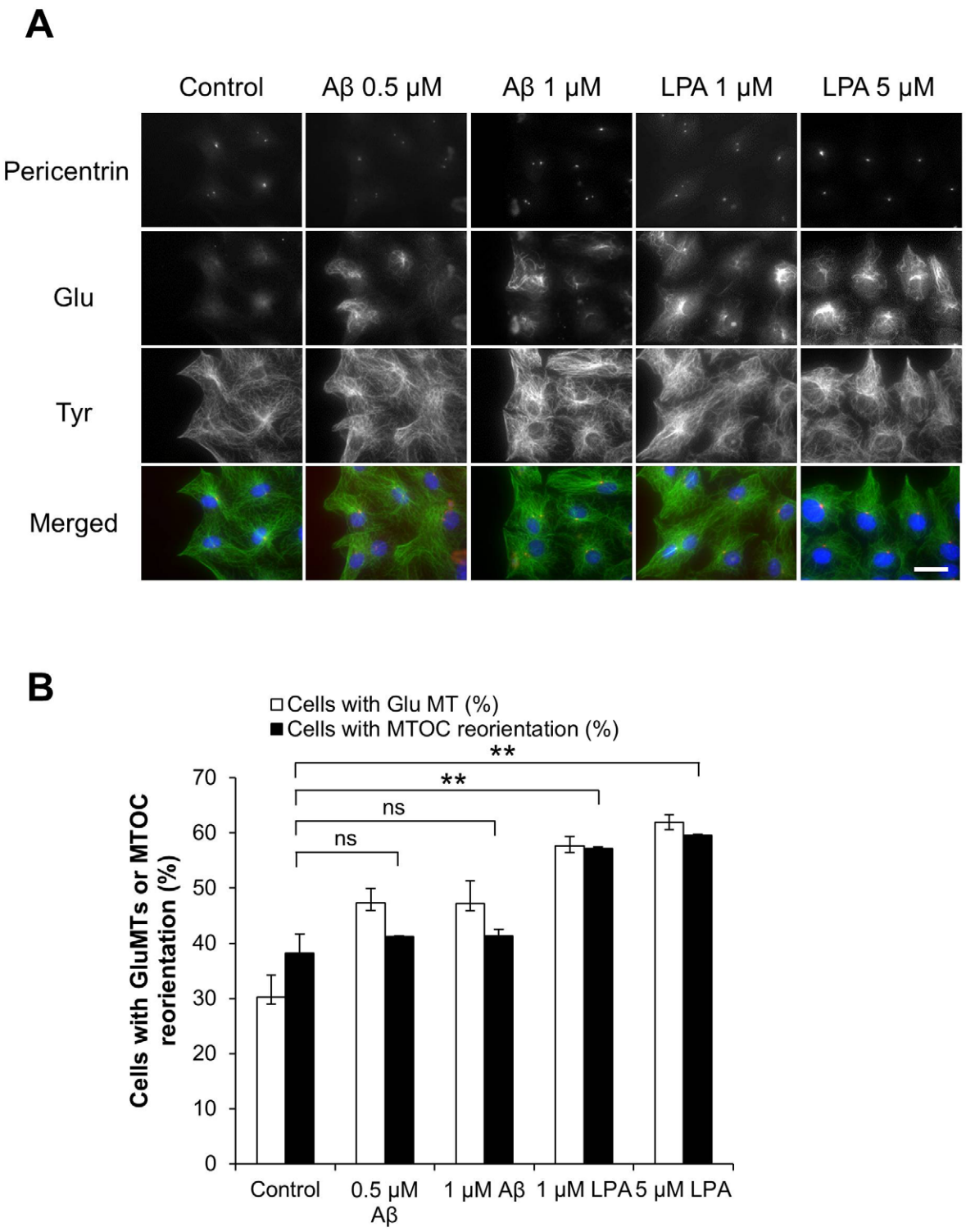

Fig. S2. Aβ does not induce reorientation of MTOC in wounded monolayers. (A) Immunostaining of detyrosinated (Glu), tyrosinated (Tyr) tubulin and pericentrin to localize the MTOC in starved cells at the wound treated with either Aβ or LPA at the indicated concentrations. (B) Quantification of the percentage of cells treated as in (A) with detyrosinated (Glu) MTs or reoriented MTOC. Data are mean ± SEM from three independent experiments (n>100 per sample in each experiment).** $p<0.01$ by Chi square test. Bar, 20 mm.

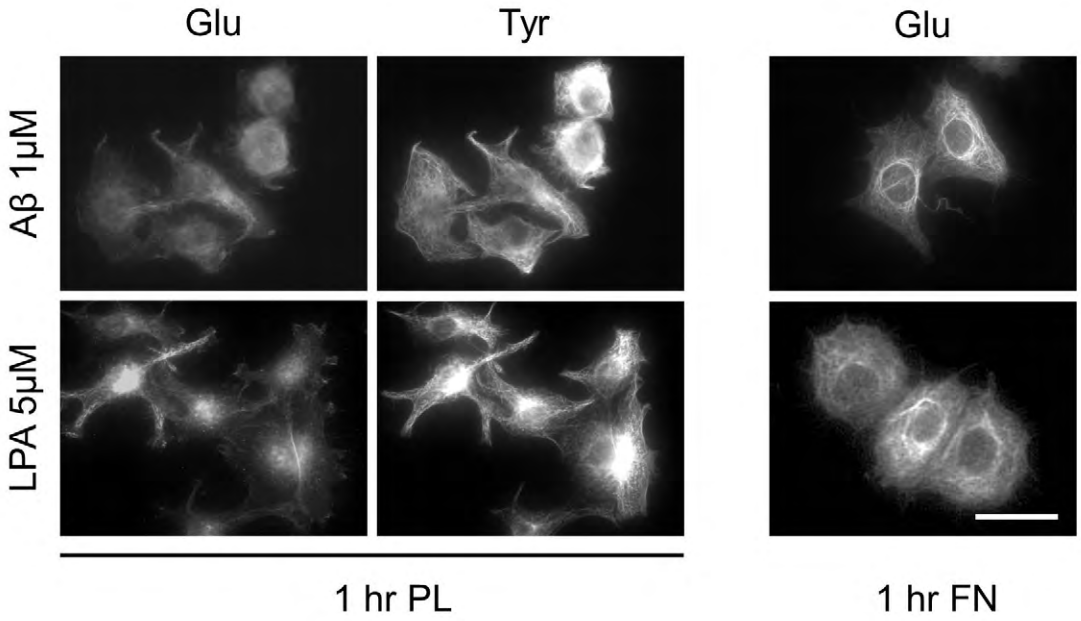

Fig. S3. Immunostaining of detyrosinated (Glu) and tyrosinated (Tyr) MTs in cells spreading on polylysine (PL) or fibronectin (FN) for 1 h while treated with Aβ or LPA. Bar, 20 mm.

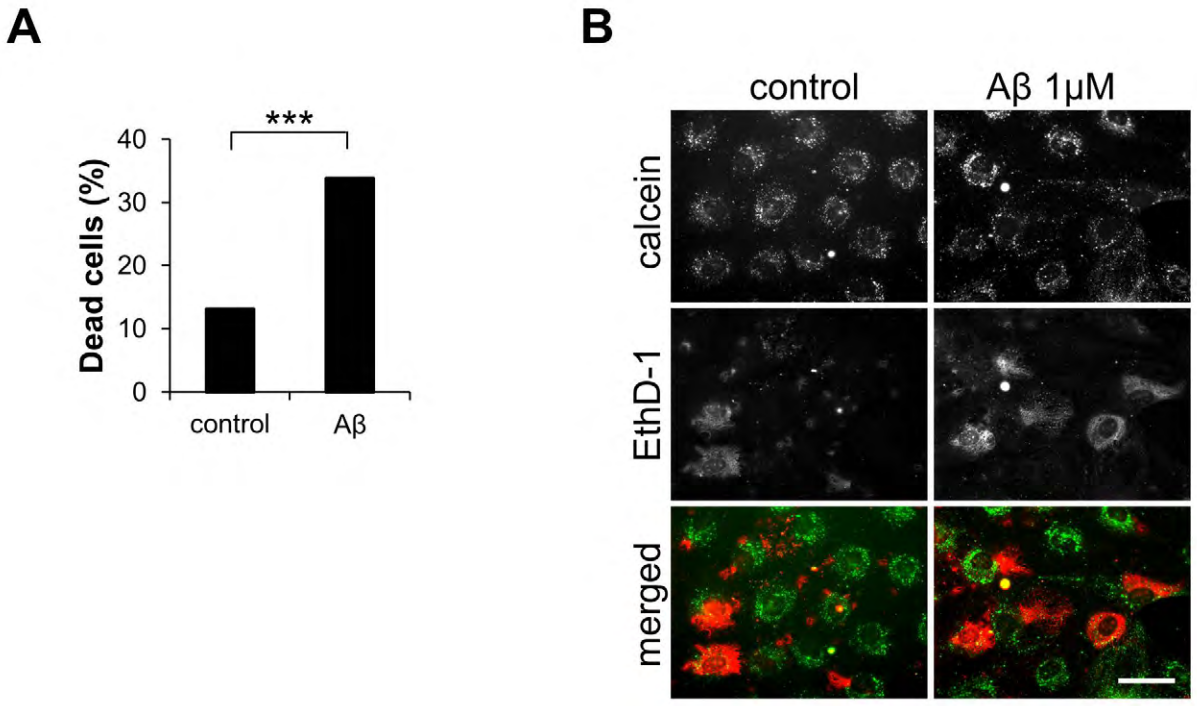

Fig. S4. Aβ induces cell death in NIH3T3 cells. (A) Quantification of the percentage of dead cells by calcein/EthD-1 fluorescence in cells treated with Aβ (1 μM) for 24 h prior to live-labeling and fixation. (B) Fluorescence images of cells treated as in (A). *** $p<0.001$ by Chi square test. Bar, 20 mm.